A Multinuclear Solid-State NMR Study of Alkali Metal Ions in Tetraphenylborate Salts, M[BPh_4] (M = Na, K, Rb and Cs): What Is the NMR Signature of Cation−π Interactions?

Gang Wu*,† and Victor Terskikh‡

Department of Chemistry, Queen's University, 90 Bader Lane, Kingston, Ontario, Canada K7L 3N6, and Steacie Institute for Molecular Sciences, National Research Council Canada, Ottawa, Canada K1A 0R6.

Received: July 22, 2008; Revised Manuscript Received: August 21, 2008

We report a multinuclear solid-state (^{23}Na, ^{39}K, ^{87}Rb, ^{133}Cs) NMR study of tetraphenylborate salts, M[BPh_4] (M = Na, K, Rb, Cs). These compounds are isostructural in the solid state with the alkali metal ion surrounded by four phenyl groups resulting in strong cation−π interactions. From analyses of solid-state NMR spectra obtained under stationary and magic-angle spinning (MAS) conditions at 11.75 and 21.15 T, we have obtained the quadrupole coupling constants, C_Q, and the chemical shift tensor parameters for the alkali metal ions in these compounds. We found that the observed quadrupole coupling constant for M^+ in M[BPh_4] is determined by a combination of nuclear quadrupole moment, Sternheimer antishielding factor, and unit cell dimensions. On the basis of a comparison between computed paramagnetic and diamagnetic contributions to the total chemical shielding values for commonly found cation−ligand interactions, we conclude that cation−π interactions give rise to significantly lower paramagnetic shielding contributions than other cation−ligand interactions. As a result, highly negative chemical shifts are expected to be the NMR signature for cations interacting exclusively with π systems.

1. Introduction

In recent years solid-state NMR spectroscopy has become a useful tool for direct detection of alkali metal ions in a variety of organic and biological systems.[1−12] One important step toward useful applications of this methodology to unknown systems is to establish relationships between NMR spectral parameters of alkali metal ions and ion binding environment. Among cation−ligand interactions, cation−π interactions are of particular importance.[13−15] Several years ago, we reported solid-state ^{23}Na and ^{39}K NMR spectra for sodium and potassium tetraphenylborates, Na[BPh_4] and K[BPh_4].[16] These compounds are classic examples containing cation−π interactions. We found that the alkali metal ions in these compounds, Na^+ and K^+, exhibit highly negative ^{23}Na and ^{39}K chemical shifts, corresponding to a highly shielded environment at the metal center. The observed highly negative chemical shifts in Na[BPh_4] and K[BPh_4] are in agreement with those reported by Schurko and co-workers[17−19] for metallocene compounds where cation−π interactions are present. As a result, we proposed that a highly shielded environment can be used as an NMR spectral signature for detecting cation−π interactions. This suggestion was further corroborated by extensive quantum chemical calculations for most common cation−π systems. Recently, Bryce and co-workers[20,21] examined several crown ether complexes containing cation−π interactions by solid-state NMR and found that the ^{23}Na and ^{39}K chemical shifts in these compounds, however, lie more or less within the normal chemical shift range. We should point out here that a fundamental difference exists between tetraphenylborates (as well as metallocene compounds) and the crown ether complexes examined by Bryce and co-workers. That is, the metal ions in these crown ether complexes are always coordinated *simultaneously* to common ligands (e.g., via oxygen and nitrogen atoms) and π systems. Regardless of this difference, a question should be raised as to how exactly the NMR parameters can be used as a practical tool for detecting cation−π interactions in systems where "mixed" cation−ligand interactions are present.

In this study, we extend our earlier study of tetraphenylborate salts to include the remaining two members of the isostructural series, Rb[BPh_4] and Cs[BPh_4]. All these tetraphenylborates, M[BPh_4] (M = Na, K, Rb, Cs), crystallize in tetragonal form with space group $I\bar{4}2m$.[16,22−24] In the crystal lattice of these compounds, each metal ion is surrounded by four phenyl groups with the distance between the metal ion and the center of the phenyl ring to be approximately 3.3−3.4 Å (see molecular structure of M[BPh_4] in Figure 1, crystallographic and nuclear data in Table 1).[25,26] Here we report an extended multinuclear solid-state NMR study (^{23}Na, ^{39}K, ^{87}Rb and ^{133}Cs) of these isostructual tetraphenylborate salts. From the experimental data, we obtain the quadrupole coupling tensors and chemical shift tensors for Na^+, K^+, Rb^+ and Cs^+ ions. We also compare the NMR spectral parameters for alkali metal ions involved in common cation−ligand interactions and cation−π interactions and address the question as to the exact NMR signature of cation−π interactions.

2. Experimental section

All crystalline tetraphenylborates were purchased from Sigma-Aldrich (Canada) and used without further purification. The crystal forms of the solid samples were confirmed using X-ray powder diffraction as described previously.[16] Solid-state ^{87}Rb and ^{133}Cs NMR spectra at 11.75 T were recorded on a Bruker Avance-500 NMR spectrometer. Solid-state ^{39}K NMR spectra at 21.15 T were recorded at the National Ultrahigh-Filed NMR Facility for Solids (Ottawa, Canada). A Bruker 4-mm MAS probe and a home-built 7 mm static probe were used. At 21.15 T, the Larmor frequency for ^{39}K is 42.0 MHz. All chemical

* Corresponding author. E-mail: gang.wu@chem.queensu.ca.
† Queen's University.
‡ National Research Council Canada.

10.1021/jp8064739 CCC: $40.75
Published on Web 09/25/2008

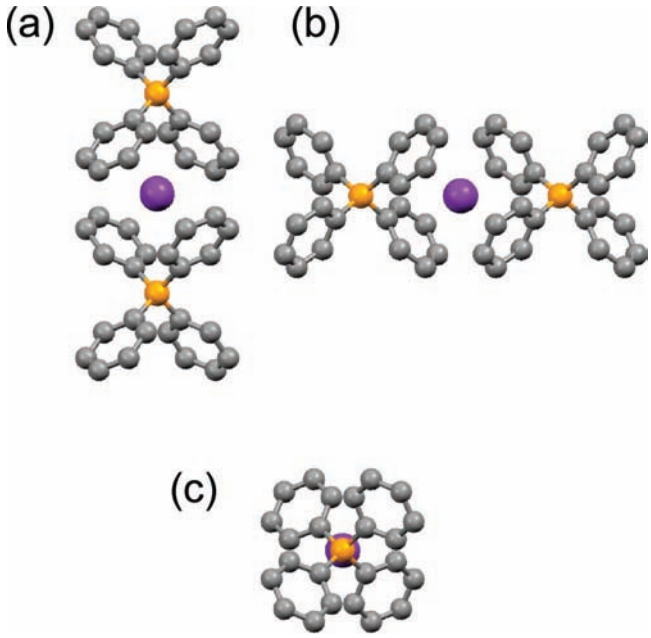

Figure 1. Partial crystal structures of M[BPh_4] viewed from (a) *a*, (b) *b*, and (c) *c* axes. Hydrogen atoms are omitted for clarity. Color code: M (purple), B (gold), C (gray).

TABLE 1: Crystallographic Unit Cell Dimensions of M[BPh_4], Nuclear Properties of Alkali Metal Ions, and Experimental NMR Quadrupole Coupling and Chemical Shift Tensors Determined for M[BPh_4]

	Na[BPh_4]	K[BPh_4]	Rb[BPh_4]	Cs[BPh_4]
Crystallographic Data				
$a = b$ (Å)	11.524[a]	11.211[a]	11.212[b]	11.1647[c]
c (Å)	7.462	7.918	8.098	8.3352
V (Å^3)	991	995	1018	1039
Nuclear Property[d]	^{23}Na	^{39}K	^{87}Rb	^{133}Cs
natural abundance/%	100	93.1	27.8	100
$\gamma/10^7$ rad T^{-1} s^{-1}	7.0801	1.2498	8.7807	3.5277
eQ/mb (1 mb = 10^{-31} m^2)	104.1	58.5	133.5	−3.43
$1 - \gamma_\infty$	6.5	22.8	53.8	111.0
Experimental Results[e]				
$\lvert C_Q \rvert$/MHz	1.24 ± 0.05	1.30 ± 0.02	6.65 ± 0.02	0.335 ± 0.002
δ_{iso}/ppm	−45.6 ± 0.5	−87 ± 2	−170 ± 2	−277 ± 2
$\delta_{11} = \delta_{22}$ /ppm	−41 ± 2	−78 ± 5	−158 ± 5	−254 ± 5
δ_{33}/ppm	−55 ± 2	−100 ± 5	−194 ± 5	−327 ± 5
$\Omega = (\delta_{11} - \delta_{33})$ /ppm	14	22	36	73

[a] From ref 16. [b] From ref 23. [c] From ref 24. [d] From refs 25 and 26. [e] The quadrupole coupling tensor is axially symmetric ($\eta_Q = 0$) and has the same orientation as the chemical shift tensor ($\alpha = \beta = \gamma = 0°$).

shifts were referenced using external samples of 1.0 M MCl(aq) in H_2O. All quantum mechanical calculations were performed using the Gaussian 98 software package[27] on a SunFire 6800 multiprocessor system (24 × 900 MHz processors and 24 GB of memory).

3. Results and Discussion

Figure 2 shows ^{39}K MAS and static spectra of K[BPh_4] at 21.1 T. Analysis of these spectra yielded the following parameters: $C_Q = 1.30 \pm 0.02$ MHz, $\eta_Q = 0$, $\delta_{iso} = -87 \pm 2$ ppm, $\delta_{11} = \delta_{22} = -78 \pm 5$ ppm, $\delta_{33} = -100 \pm 5$ ppm. The ^{39}K quadrupole parameters are in agreement with those reported in our earlier study;[16] however, here for the first time we are able to report an accurate ^{39}K chemical shift tensor for K[BPh_4]. The axial symmetry observed for both ^{39}K quadrupole coupling and chemical shift tensors is consistent with the site symmetry

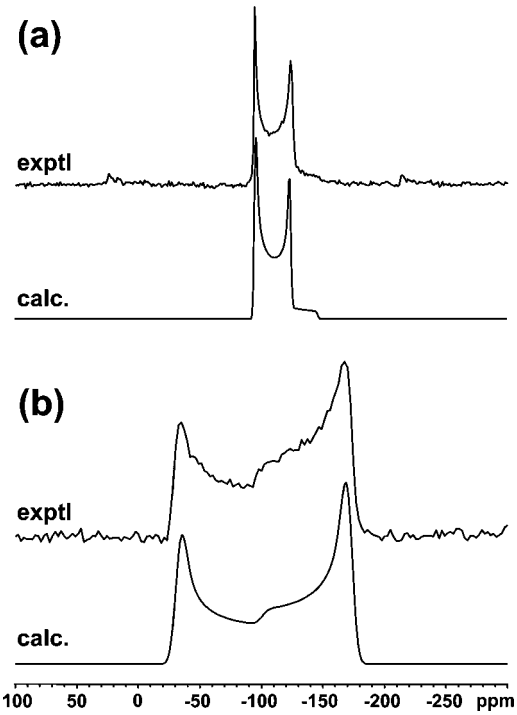

Figure 2. Experimental and simulated ^{39}K NMR spectra of K[BPh_4] at 21.15 T. The following experimental parameters were used: (a) MAS, sample spinning 5 kHz, 30 s recycle delay, 1500 transients; (b) static, 30 s recycle time, 1500 transients.

in this compound. In fact, this axial symmetry is true at the metal center in all tetraphenylborates studied here. The observed span of the ^{39}K chemical shift anisotropy, $\Omega = \delta_{11} - \delta_{33} = 22$ ppm, is similar to those found in inorganic salts,[28] but somewhat smaller than those found in a K^+−crown ether complex, as well as diatomic molecules $^{39}K^{19}F$ and $^{39}K^{35}Cl$.[21]

Figure 3 shows ^{87}Rb MAS and static spectra of Rb[BPh_4] at 11.75 T. The ^{87}Rb quadrupole coupling constant found for Rb[BPh_4] is 6.65 MHz. The isotropic ^{87}Rb chemical shift, −170 ppm, is also rather negative compared with other Rb^+ salts. This is in agreement with the findings in ^{23}Na and ^{39}K chemical shifts in tetraphenylborates. The ^{87}Rb chemical shift tensor was also determined for Rb[BPh_4]: $\delta_{11} = \delta_{22} = -158 \pm 5$ ppm, $\delta_{33} = -194 \pm 5$ ppm. The span of the ^{87}Rb chemical shift anisotropy, $\Omega = \delta_{11} - \delta_{33} = 36$ ppm, is comparable to those found in Rb^+ salts.[29]

Figure 4 shows ^{133}Cs MAS and static spectra of Cs[BPh_4]. The observed ^{133}Cs MAS spectrum is typical of Cs compounds where a large number of sharp spinning sidebands are present due to satellite transitions. Because ^{133}Cs has a very small quadrupole moment, the second-order quadrupole broadening is negligible at the magnetic field strength of 11.75 T employed in this study. However, both ^{133}Cs quadrupole coupling and chemical shift tensors can be readily obtained from an analysis of the static spectrum. The observed ^{133}Cs quadrupole coupling constant is 0.335 MHz. The isotropic ^{133}Cs chemical shift is also rather negative, −277 ppm, consistent with our observation for all tetraphenylborates. The span of the ^{133}Cs chemical shift anisotropy, $\Omega = \delta_{11} - \delta_{33} = 73$ ppm, is similar to those in Cs^+ salts.[30,31] It is also quite interesting to note that the ^{133}Cs NMR parameters found for Cs[BPh_4] are similar to those reported by Gullion and co-workers for [Cs(*p-tert*-butylcalix[4]-arene-H)(MeCN)], $C_Q = 0.245$ MHz and $\delta_{iso} = -256$ ppm.[32] This is entirely consistent with the fact that the Cs ion in this guest−host compound is also involved in strong cation−π interactions.

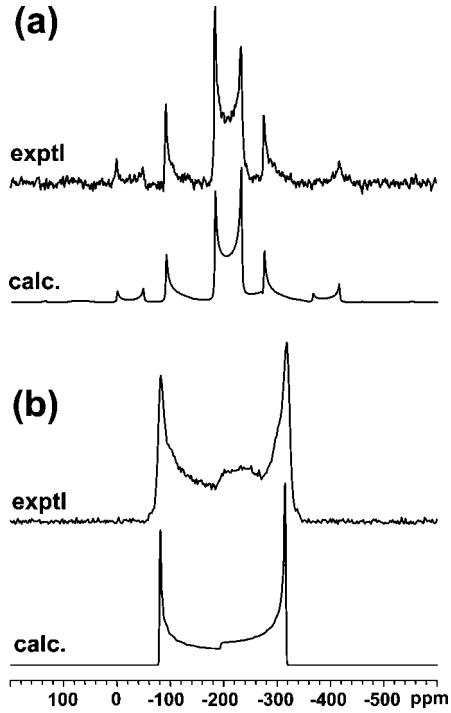

Figure 3. Experimental and simulated ^{87}Rb NMR spectra of Rb[BPh$_4$] at 11.75 T. The following experimental parameters were used: (a) MAS, sample spinning 15 kHz, 2 s recycle time, 3280 transients; (b) stationary, 5 s recycle time, 12 322 transients. The ^{1}H decoupling RF field was approximately 90 kHz.

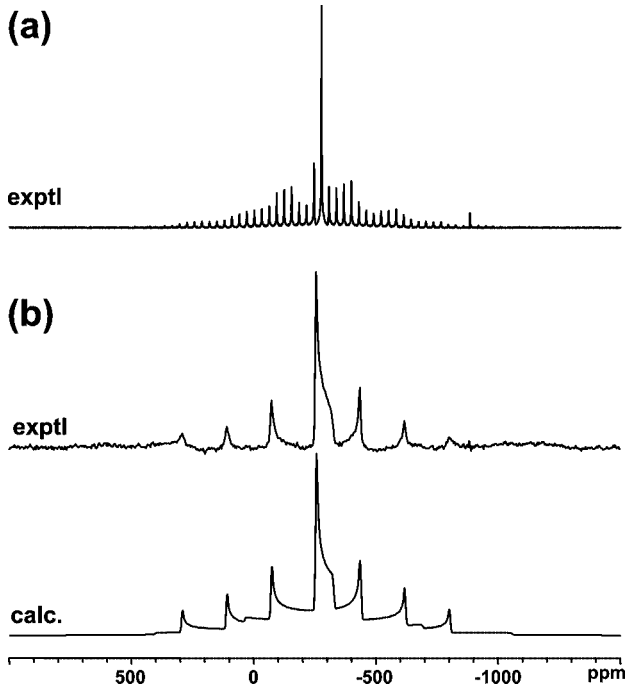

Figure 4. Experimental and simulated ^{133}Cs NMR spectra of Cs[BPh$_4$] at 11.75 T. The following experimental parameters were used: (a) MAS, sample spinning 10 kHz, 60 s recycle delay, 80 transients; (b) static, 30 s recycle time, 3774 transients.

Table 1 summarizes the solid-state NMR results determined for all four M[BPh$_4$] compounds (M = Na, K, Rb, Cs). The quadrupole coupling constants for M[BPh$_4$] also provide a good example to illustrate how the values of C_Q for different nuclides should be compared within a series of the isostructural compounds. Very often when comparing line broadening factors between different quadrupolar nuclei, one common

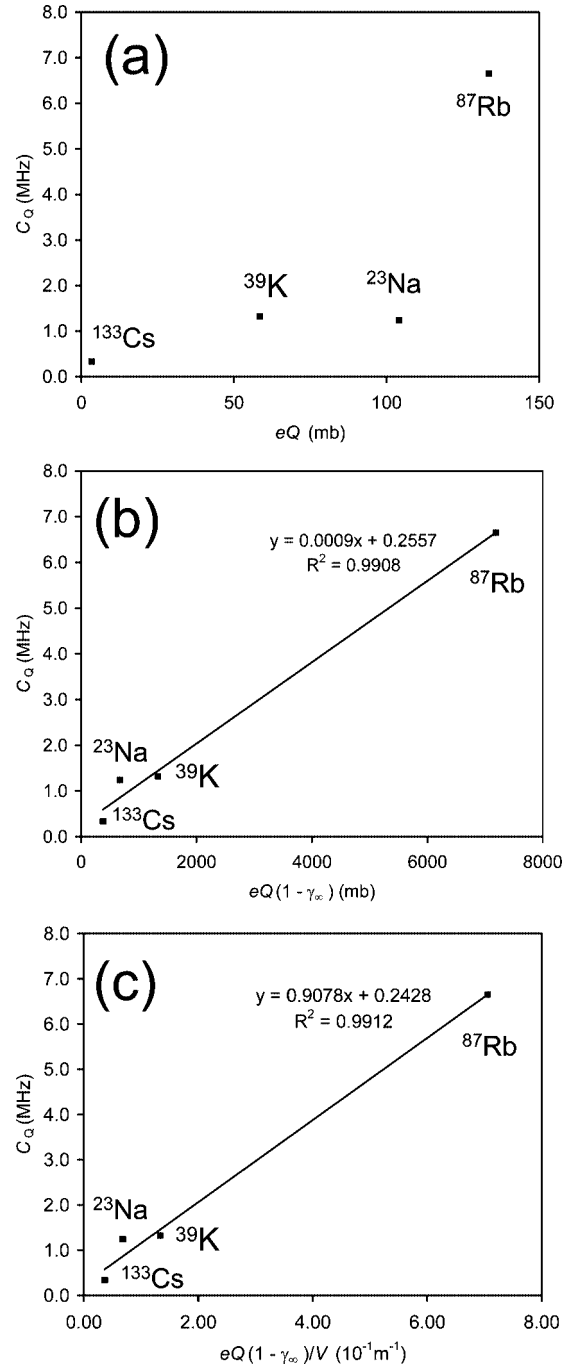

Figure 5. Dependence of C_Q observed for M^+ in M[BPh$_4$] (M = Na, K, Rb, Cs) on (a) eQ, (b) $eQ(1 - \gamma_\infty)$, and (c) $eQ(1 - \gamma_\infty)/V$, where V refers to the unit cell volume (see Table 1).

mistake is to use the value of quadrupole moment (eQ) alone as an indicator of quadrupole line broadening. In fact, it is the product of eQ and the Sternheimer antishielding factor (γ_∞)[33−37] that determines the magnitude of C_Q observed in NMR experiments for a particular metal ion. The nuclear quadrupole coupling constant C_Q is defined as

$$C_Q = \frac{e^2 q_{obs} Q}{h} \quad (1)$$

where eQ is the nuclear quadrupole moment, and $eq_{obs} = V_{ZZ}$ is the largest principal value of the electric field gradient tensor observed at the nucleus. Contributions from the inner closed

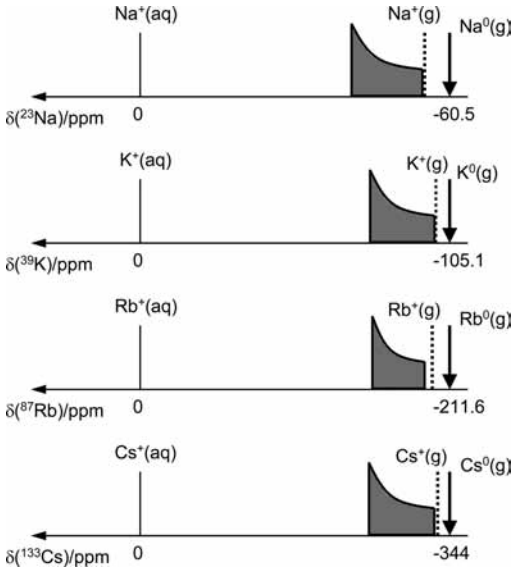

Figure 6. Illustration of the relationship between the chemical shift tensor components observed for the M^+ ions in $M[BPh_4]$ (M = Na, K, Rb, Cs) (shaded areas) and the chemical shifts for M^+(aq), M^+(g), and M^0(g). See text for discussion.

TABLE 2: Theoretical Chemical Shielding Values in Parts Per Million for Alkali Metals (M^+ and M^0) in the Gas Phase

	Hartree−Fock[a]			relativistic[b]		
M	$\sigma(M^+)$	$\sigma(M^0)$	$\Delta\sigma$	$\sigma(M^+)$	$\sigma(M^0)$	$\Delta\sigma$
Li	95.404	101.450	6.046	95.5	101.5	6.0
Na	623.805	628.894	5.089	632.2	637.1	4.9
K	1325.421	1329.354	3.933	1371	1376	5
Rb	3363.200	3366.793	3.593	3748	3760	12
Cs	5777.031	5780.199	3.169	7267	7280	13

[a] From ref 37. [b] From ref 38. $\Delta\sigma = \sigma(M^0) - \sigma(M^+)$.

electron shells to the observed electric field gradient are expressed via the Sternheimer antishielding factor, γ_∞, as

$$eq_{obs} = (1 - \gamma_\infty)eq_{ionic} \quad (2)$$

where eq_{ionic} is the electric field gradient due to surrounding ionic charges. As seen from Table 1, the value of $(1 - \gamma_\infty)$ can be quite large, especially for heavy atoms. Figure 5 illustrates the dependence of C_Q on eQ and $eQ(1 - \gamma_\infty)$. Within the isostructural compounds, the unit cell size also plays a role because the electric field gradient arising from the lattice is scaled by the unit cell volume. As seen in Figure 5, when all these factors are considered, the values of C_Q for ^{23}Na, ^{39}K, ^{87}Rb and ^{133}Cs nuclei are nicely correlated with $eQ(1 - \gamma_\infty)/V$, where V is the unit cell volume. Using the data given in Table 1, we obtain the values of $eQ(1 - \gamma_\infty)$ to be 677, 1334, 7182, and 381 mb for ^{23}Na, ^{39}K, ^{87}Rb, and ^{133}Cs nuclei, respectively. This suggests that ^{87}Rb would experience the most significant quadrupole broadening. The line width of the central transition shows an even stronger dependence on γ_∞, (i.e., proportional to $[eQ(1 - \gamma_\infty)]^2/\gamma$). For example, this quantity is 0.7, 15, 57, and 0.4×10^{-50} m^4 rad^{-1} T s for ^{23}Na, ^{39}K, ^{87}Rb and ^{133}Cs, respectively. This illustrates why, at a given magnetic field, solid-state ^{87}Rb and ^{39}K NMR signals are so much broader than ^{23}Na and ^{133}Cs NMR signals for cations in similar environments of surrounding ionic charges.

General Trends of Chemical Shifts within the Alkali Metal Group. It is clear from the above discussion that a common feature of the ^{23}Na, ^{39}K, ^{87}Rb and ^{133}Cs chemical shifts in $M[BPh_4]$ (M = Na, K, Rb, Cs) is the fact that their values are quite negative compared with those from other salts. In this section, we further examine these chemical shift tensors within the alkali metal group. To understand chemical shifts from different nuclei, we can use the chemical shifts of their respective free atoms as a starting reference point. Fortunately, for alkali metals, the chemical shielding difference between M^+(aq) (common chemical shift reference) and M^0(g) (free alkali metal atoms in the gas phase) has been experimentally determined by either atomic beam magnetic resonance or optical pumping experiments[38] (see Figure 6). However, M^0(g) is not a perfect reference point because we are dealing with alkali metal ions, M^+. So, what are the chemical shift values for M^+(g) (free alkali metal ions in the gas phase)? In the literature, there are several experimental studies that reported the chemical shielding difference between M^+(g) and M^0(g) for alkali metals.[39−41] The accuracy of these experiments was later questioned by Pyper.[42] In the absence of new more reliable experimental data, it is reasonable for us to rely on highly accurate quantum chemical calculations to provide estimated chemical shifts for M^+(g). Table 2 lists computed chemical shielding values for M^0(g) and M^+(g) at the Hartree−Fock[42] and the relativistic random-phase approximation (RRPA)[43] levels. As seen from Table 2, although the Hartree−Fock method somewhat underestimates the chemical shielding for heavy atoms such as Rb and Cs, the chemical shielding differences for M^0(g) and M^+(g) are generally predicted reliably to be within a few parts per million by both methods. In Figure 6, the chemical shift values of M^+(g) are marked using the results from relativistic calculations of Johnson et al.[43] In general, the total chemical shielding at a nucleus (σ) can be separated into two parts: paramagnetic (σ_p) and diamagnetic (σ_d) contributions:[44,45]

$$\sigma = \sigma_p + \sigma_d \quad (3)$$

Because the only contribution to the chemical shielding of M^+(g) is the diamagnetic contribution, the chemical shielding

TABLE 3: Computed HF/6-311++G(d,p) ^{23}Na Isotropic Chemical Shielding Values in Various Na−Ligand Systems

Na^+−ligand system	Na−X/Å[a]	σ_p/ppm	σ_d/ppm	σ_{total}/ppm
$Na^+-\pi$				
furan	2.533	−3.1	627.1	624.0
pyrrole	2.492	−6.5	627.4	620.9
benzene	2.432	−4.1	627.1	623.0
tryptophan	2.328	−5.1	629.4	624.3
tyrosine	2.412	−5.7	629.3	623.6
uracil	2.693	−4.8	625.9	621.1
guanine	2.475	−3.9	627.1	623.2
Na^+−O				
water	2.118	−24.5	625.1	600.6
acetone	2.131	−20.4	625.0	604.6
dimethylether	2.095	−25.4	626.1	600.7
methylacetate	2.024	−27.4	626.5	599.1
formamide	2.026	−27.2	626.4	599.2
nitromethane (bidentate mode)	2.306	−26.2	625.9	599.7
Na^+−N				
ammonia	2.318	−31.7	625.3	593.6
trimethylammonia	2.258	−27.7	625.3	597.6
Na^+−S				
Me−S−Me	2.707	−23.8	625.8	602.0
thioacetone	2.680	−19.2	627.2	608.0
HS−Me	2.817	−24.4	625.5	601.1

[a] X refers to the centroid point in $Na^+-\pi$ systems and the ligand atoms of O, N, and S in other systems.

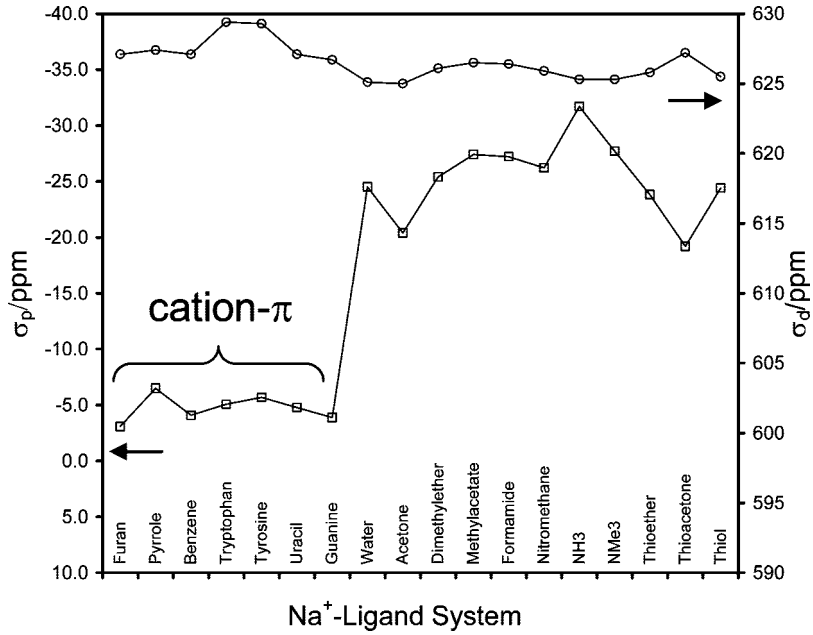

Figure 7. Dependence of the paramagnetic and diamagnetic contributions to the total ^{23}Na chemical shielding values on the nature of Na^+−ligand interactions.

value for M^+(g) is the largest possible (at the upper limit) that can be observed for M^+. It is significant to note in Figure 6 that the chemical shift of the alkali metal cation along the crystallographic *c*-axis (the direction of δ_{33}) of $M[BPh_4]$ is close to the value found for M^+(g). This means that the paramagnetic contribution is essentially zero when the external magnetic field is along this direction of the $M[BPh_4]$ crystals. This can be understood on the basis of directional dependence of the chemical shift. As we demonstrated previously, the paramagnetic contribution to the chemical shielding at the metal nucleus is the largest when the external magnetic field is *parallel* to the π plane (the directions of the δ_{11} and δ_{22} components).[16] As seen from Figure 1, when the magnetic field is along the *c* axis, it can be considered to be approximately *perpendicular* to all four phenyl planes. As a result, there is essentially no paramagnetic contribution to the metal shielding when the magnetic field is along *c* axis. On the other hand, when the magnetic field is along either the *a* or *b* axis, the four phenyl planes are more or less *parallel* to the external field, resulting in significant paramagnetic contributions. Under such a circumstance, the chemical shift anisotropy provides a good measure of the paramagnetic shielding contribution in each of $M[BPh_4]$ salts. As seen from the results shown in Table 1, the paramagnetic shielding contribution increases with the atomic number, *Z*, down the alkali metal group. This is in line with the general *Z* dependence of chemical shielding discovered by Jameson and Gutowsky.[46]

What Is the True NMR Signature of Cation−π Interactions? As mentioned earlier, there are some seemingly contradictory observations regarding to the actual chemical shifts for an alkali metal ion that is involved in cation−π interactions. In the previous section, we have shown that the highly negative chemical shifts observed in $M[BPh_4]$ are due to the minimal paramagnetic shielding contribution experienced by the metal ion in this system. It is also clear that, when an alkali metal ion is involved in coordination with "mixed" ligands, the total chemical shielding of the metal ion depends on the sum of all paramagnetic shielding contributions from different ligand groups. Thus it makes little sense to directly compare chemical shifts observed for "pure" cation−π systems (e.g., tetraphenylborates, calix[4]arenes, and metallocenes) with those for systems containing "mixed" ligands. Table 3 shows computed paramagnetic and diamagnetic contributions to the total ^{23}Na chemical shielding for common Na−ligand interactions. As shown in Figure 7, one can clearly see that the paramagnetic shielding contributions to ^{23}Na chemical shielding from cation−π interactions are indeed distinctly smaller than those from other ligands by ca. 20 ppm. This is in agreement with our previous suggestion to use this feature as the NMR signature of cation−π interactions.[16] However, this does not mean that the chemical shifts for an alkali metal ion would *always* be highly shielded when it is involved in cation−π interactions. In systems containing "mixed" ligands, this NMR signature means that the alkali metal ion would become less shielded if the π-ligand were to be replaced by a different ligand. This may explain why Bryce and co-workers[20,21] observed somewhat "normal" ^{23}Na and ^{39}K chemical shifts in crown ether complexes containing cation−π interactions.

4. Conclusion

We have reported solid-state ^{39}K, ^{87}Rb, and ^{133}Cs NMR spectra for $M[BPh_4]$ (M = K, Rb, Cs) obtained at 11.75 and 21.15 T. In all these cases, we were able to determine both quadrupole coupling and chemical shift tensors. Combining with data reported previously, we found that the observed quadrupole coupling constants for ^{23}Na, ^{39}K, ^{87}Rb, and ^{133}Cs show an excellent correlation with the values of $eQ(1 - \gamma_\infty)/V$ within these isostructural compounds. For $M[BPh_4]$, we also found that the paramagnetic shielding contribution is essentially zero when the external magnetic field is along the crystallographic *c*-axis of the tetragonal lattice. The chemical shift anisotropy at the alkali metal ion is due to paramagnetic shielding contributions along the crystallographic *a*- and *b*-axes, which also show a clear *Z* dependence. Here we confirm that the NMR signature of cation−π interactions is indeed associated with the fact that the paramagnetic shielding contributions are distinctly smaller than those from other ligands. Consequently, highly negative chemical shifts are associated with cations interacting exclusively with π-systems. However, caution should be exercised

when one deals with systems containing "mixed" ligands, because the observed chemical shift for the alkali metal ion is a sum of shielding contributions from all ligands.

Acknowledgment. This work was supported by grants from the Natural Sciences and Engineering Research Council (NSERC) of Canada. All quantum mechanical calculations were performed at the High Performance Computing Virtual Laboratory (HPCVL) at Queen's University. Access to the 900 MHz NMR spectrometer was provided by the National Ultrahigh Field NMR Facility for Solids (Ottawa, Canada), a national research facility funded by the Canada Foundation for Innovation, the Ontario Innovation Trust, Recherche Québec, the National Research Council Canada, and Bruker BioSpin and managed by the University of Ottawa (www.nmr900.ca). The NSERC is acknowledged for a Major Resources Support grant.

References and Notes

(1) Wu, G. *Biochem. Cell Biol.* **1998**, *76*, 429.
(2) Wong, A.; Sham, S.; Wang, S. N.; Wu, G. *Can. J. Chem.* **2000**, *78*, 975.
(3) Wong, A.; Wu, G. *J. Phys. Chem. A* **2000**, *104*, 11844.
(4) Tossell, J. A. *J. Phys. Chem. B* **2001**, *105*, 11060.
(5) Grinshtein, J.; Grant, C. V.; Frydman, L. *J. Am. Chem. Soc.* **2002**, *124*, 13344.
(6) Madeddu, M. *Solid State Nucl. Magn. Reson.* **2002**, *22*, 83.
(7) Wong, A.; Wu, G. *J. Am. Chem. Soc.* **2003**, *125*, 13895.
(8) Wu, G.; Wong, A.; Gan, Z. H.; Davis, J. T. *J. Am. Chem. Soc.* **2003**, *125*, 7182.
(9) Jost, S.; Gunther, H. *Magn. Reson. Chem.* **2003**, *41*, 373.
(10) Wu, G.; Wong, A. Solid-state nuclear magnetic resonance studies of alkali metal ions in nucleic acids and related systems. In *NMR Spectroscopy of Biological Solids*; Ramamoorthy, A., Ed.; CRC Press: Boca Raton, FL, 2006; p 317.
(11) Grant, C. V.; McElheny, D.; Frydman, V.; Frydman, L. *Magn. Reson. Chem.* **2006**, *44*, 366.
(12) Ida, R.; Wu, G. *J. Am. Chem. Soc.* **2008**, *130*, 3590.
(13) Dougherty, D. A. *Science* **1996**, *271*, 163.
(14) Ma, J. C.; Dougherty, D. A. *Chem. Rev.* **1997**, *97*, 1303.
(15) Gokel, G. W.; Barbour, L. J.; De Wall, S. L.; Meadows, E. S. *Coord. Chem. Rev.* **2001**, *222*, 127.
(16) Wong, A.; Whitehead, R. D.; Gan, Z.; Wu, G. *J. Phys. Chem. A* **2004**, *108*, 10551.
(17) Willans, M. J.; Schurko, R. W. *J. Phys. Chem. B* **2003**, *107*, 5144.
(18) Widdifield, C. M.; Schurko, R. W. *J. Phys. Chem. A* **2005**, *109*, 6865.
(19) Widdifield, C. M.; Tang, J. A.; Macdonald, C. L. B.; Schurko, R. W. *Magn. Reson. Chem.* **2007**, *45*, S116.
(20) Bryce, D. L.; Adiga, S.; Elliott, E. K.; Gokel, G. W. *J. Phys. Chem. A* **2006**, *110*, 13568.
(21) Lee, P. K.; Chapman, R. P.; Zhang, L.; Hu, J.; Barbour, L. J.; Elliott, E. K.; Gokel, G. W.; Bryce, D. L. *J. Phys. Chem. A* **2007**, *111*, 12859.
(22) Horffmann, K.; Weiss, E. *J. Organomet. Chem.* **1974**, *67*, 221.
(23) Pajzderska, A.; Maluszynska, H.; Wasicki, J. *Z. Naturforsch. A* **2002**, *57*, 847.
(24) Bryan, J. C. *Z. Kristallogr.* **2000**, *215*, 621.
(25) Pyykko, P. *Mol. Phys.* **2001**, *99*, 1617.
(26) Mackenzie, K. J. D.; Smith, M. E. *Multinuclear Solid-State NMR of Inorganic Materials*; Elsevier Science, Ltd: Amsterdam, 2002.
(27) Frisch, M. J.; Trucks, G. W.; Schlegel, H. B.; Scuseria, G. E.; Robb, M. A.; Cheeseman, J. R.; Zakrzewski, V. G.; Montgomery, J. A., Jr.; Stratmann, R. E.; Burant, J. C.; Dapprich, S.; Millam, J. M.; Daniels, A. D.; Kudin, K. N.; Strain, M. C.; Farkas, O.; Tomasi, J.; Barone, V.; Cossi, M.; Cammi, R.; Mennucci, B.; Pomelli, C.; Adamo, C.; Clifford, S.; Ochtersk, J.; Petersson, G. A.; Ayala, P. Y.; Cui, Q.; Morokuma, K.; Malick, D. K.; Rabuck, A. D.; Raghavachari, K.; Foresman, J. B.; Cioslowski, J.; Ortiz, J. V.; Stefanov, B. B.; Liu, G.; Liashenko, A.; Piskorz, P.; Komaromi, I.; Gomperts, R.; Martin, R. L.; Fox, D. J.; Keith, T.; Al-Laham, M. A.; Peng, C. Y.; Nanayakkara, A.; Gonzalez, C.; Challacombe, M.; Gill, P. M. W.; Johnson, B. G.; Chen, W.; Wong, M. W.; Andres, J. L.; Head-Gordon, M.; Replogle, E. S.; Pople, J. A. *Gaussian 98, revision A.9*; Gaussian, Inc.: Pittsburgh, PA, 1998.
(28) Moudrakovski, I. L.; Ripmeester, J. A. *J. Phys. Chem. B* **2007**, *111*, 491.
(29) Cheng, J. T.; Edwards, J. C.; Ellis, P. D. *J. Phys. Chem.* **1990**, *94*, 553.
(30) Mooibroek, S.; Wasylishen, R. E.; Dickson, R.; Facey, G.; Pettitt, B. A. *J. Magn. Reson.* **1986**, *66*, 542.
(31) Power, W. P.; Wasylishen, R. E.; Mooibroek, S.; Pettitt, B. A.; Danchura, W. *J. Phys. Chem.* **1990**, *94*, 591.
(32) Hughes, E.; Jordan, J.; Gullion, T. *J. Phys. Chem. B* **2001**, *105*, 5887.
(33) Sternheimer, R. *Phys. Rev.* **1950**, *80*, 102.
(34) Sternheimer, R. *Phys. Rev.* **1951**, *84*, 244.
(35) Lucken, E. A. C. *Nuclear Quadrupole Coupling Constants*; Academic Press: New York, 1969.
(36) Smith, J. A. S. *J. Chem. Educ.* **1971**, *48*, 39.
(37) Schmidt, P. C.; Sen, K. D.; Das, T. P.; Weiss, A. *Phys. Rev. B* **1980**, *22*, 4167.
(38) Jameson, C. J.; Mason, J. In *Multinuclear NMR*; Mason, J., Ed.; Plenum Press: New York, 1987; *Chapter 3*.
(39) Davis, S. J.; Wright, J. J.; Balling, L. C. *Phys. Rev. A* **1974**, *9*, 1494.
(40) Oluwole, A. F. *Phys. Scr.* **1977**, *15*, 339.
(41) Obiajunwa, E. I.; Adebiyi, S. A.; Togun, E. A.; Oluwole, A. F. *J. Phys. B: At. Mol. Phys.* **1983**, *16*, 2733.
(42) Pyper, N. C. *J. Phys. B: At. Mol. Phys.* **1985**, *18*, 1317.
(43) Johnson, W. R.; Kolb, D.; Hunag, K.-N. *At. Data Nucl. Data Tables* **1983**, *28*, 333.
(44) Ramsey, N. F. *Phys. Rev.* **1950**, *78*, 699.
(45) Ramsey, N. F. *Phys. Rev.* **1951**, *83*, 540.
(46) Jameson, C. J.; Gutowsky, H. S. *J. Chem. Phys.* **1964**, *40*, 1714.

JP8064739